

Mechanistic investigation of pore structure evolution in fine-grained soils subjected to chemical alteration and wetting–drying cycles



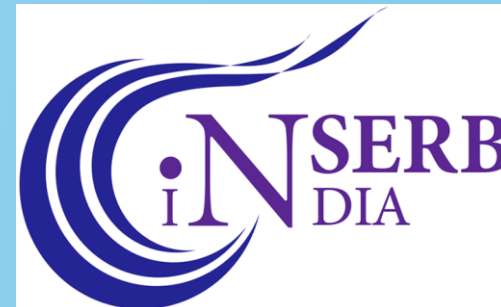
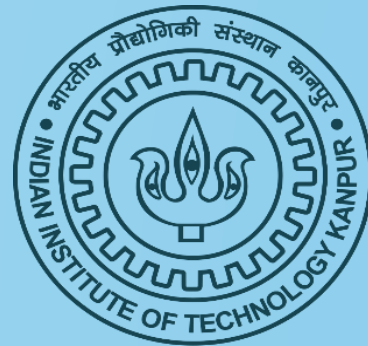
Presented by:

Mohd Sameer Alam

Research Scholar Department of Civil
Engineering

Indian Institute of Technology Kanpur

Email- sameeralam22@iitk.ac.in



Supervisor:

Professor Arghya Das

FB 304, Department of Civil Engineering
Indian Institute of Technology Kanpur

T: +91 512 259 6978

Email- arghya@iitk.ac.in



Introduction

Motivation

Methodology

Results and Discussion

References

INTRODUCTION:

- Fine-grained soils (especially clays) exhibit **complex pore structures** that strongly influence their mechanical and hydraulic behavior.
- These soils are frequently subjected to **environmental processes** such as
 - chemical alteration (e.g., salinity, contaminants)
 - cyclic wetting–drying.
- Such processes lead to **microstructural changes**, including:
 - rearrangement of clay particles
 - pore redistribution (micro → macro pores)
 - development of cracks and fissures

Therefore, a detailed investigation of pore structure evolution is essential for predicting the long-term performance of fine-grained soils in geo-environmental applications.



Fig.1 Dried clay surface exhibiting a network of desiccation cracks, a common phenomenon observed in fine-grained soils such as clays when they undergo drying.

Source-<https://eos.com/blog/soil-salinization>



Fig.2 Desiccation cracks developed in fine-grained soil following wetting–drying cycles

INTRODUCTION:

Pore structure: The pore structure in geomaterial is complex, especially in clays, and plays a critical role in controlling the mechanical, hydraulic, and chemical behavior of these fine-grained soils.

Why are clays so unique? The answer lies in their pores—**tiny, complex spaces** that control how water moves, how stress is distributed, and how the material reacts to the environment.

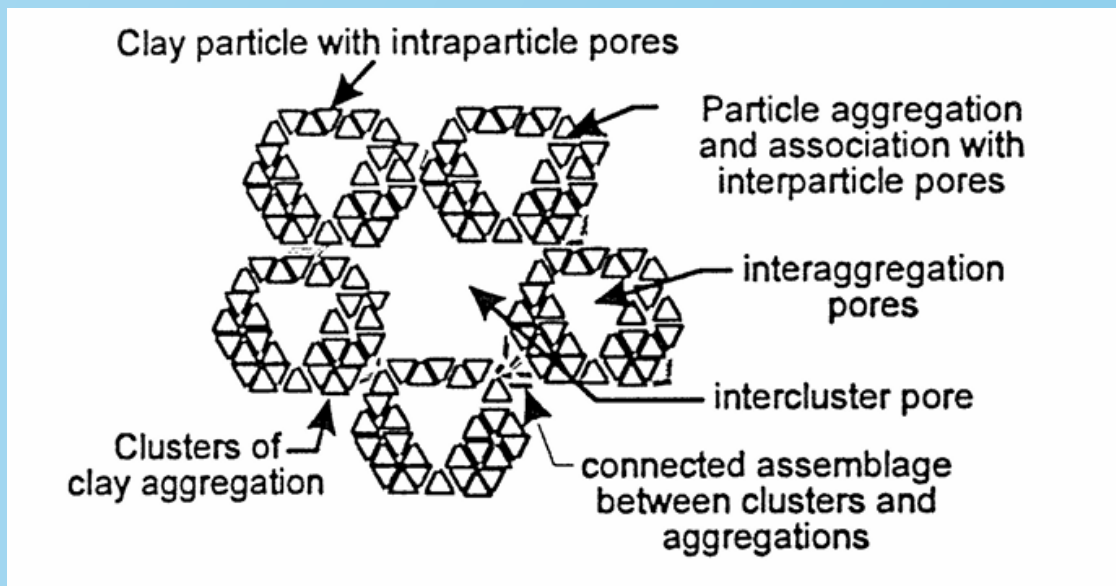


Fig. Structural elements and pore types (modified from Shear et al., 1993)

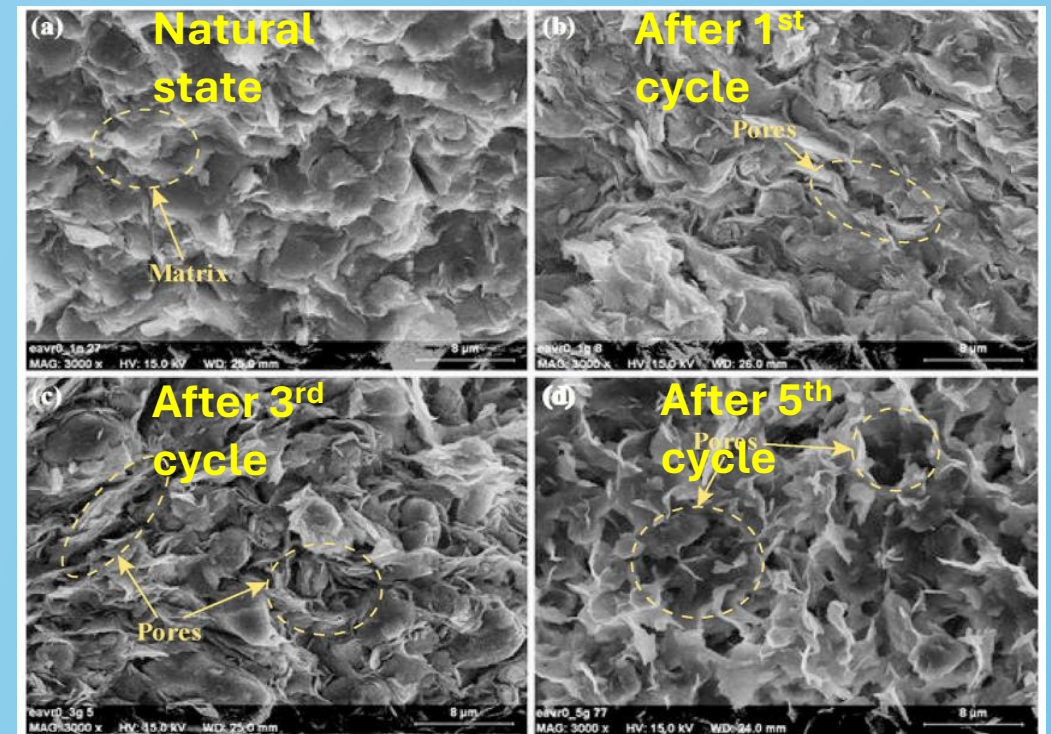


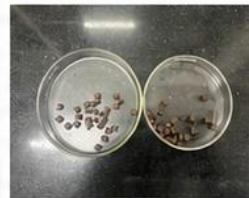
Fig. SEM micrographs from Basma et al., 1996

METHODOLOGY:

1. SAMPLE PREPARATION



Silicon Mould



Bentonite Clay



Kaolinite Clay

2. DRYING PROCESS

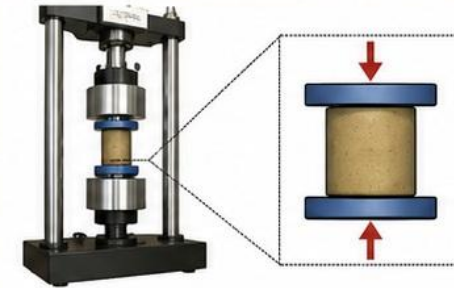


Freeze Dryer



Oven Dryer

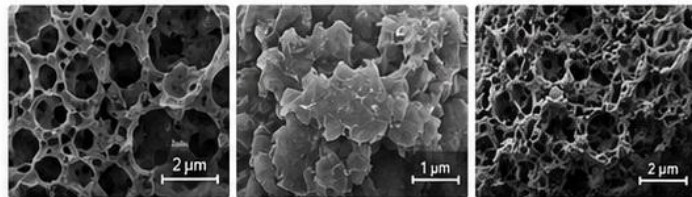
3. SAMPLE LOADING



Samples prepared and loaded to different stresses

- Loading to stress
- Ethyl alcohol added for stiffness

6. IMAGE ANALYSIS



- Pore size distribution
- Pore shape and connectivity
- Quantitative analysis of microstructural evolution

5. SEM IMAGING



Scanning Electron Microscope

4. SAMPLE PREPARATION FOR SEM



Loaded Samples



Gold Coating



Mounting on Stub



METHODOLOGY:

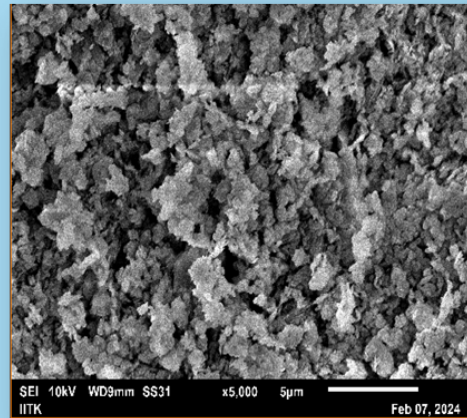


Image Filtration

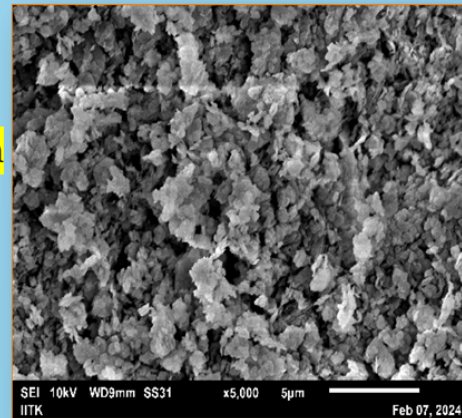
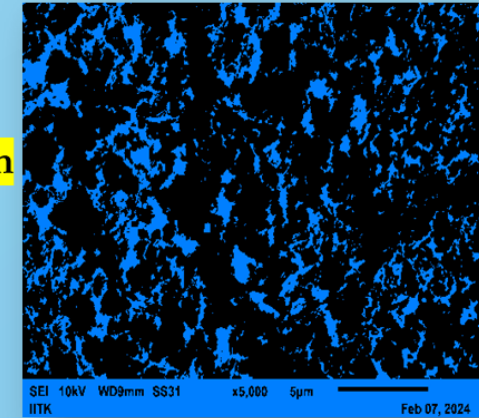


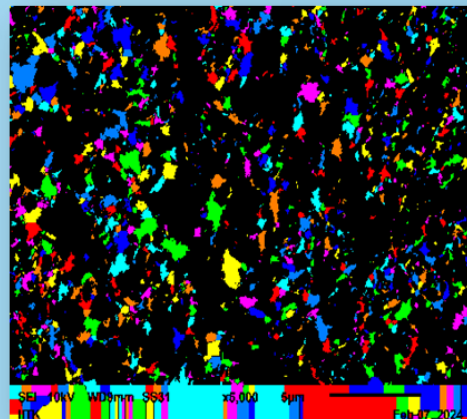
Image Binarization



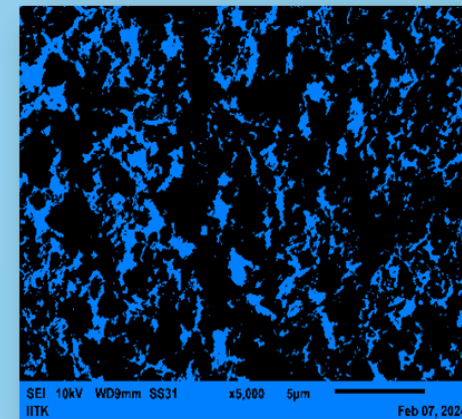
Collections of varying pores of different sizes

Blue pixels represent pores and black represents soil particles

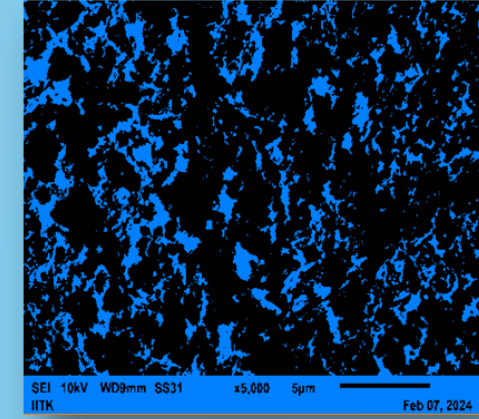
Closings of pores



Measure



Pores Separation





METHODOLOGY: Three parameters are calculated using image processing software MIPAR:

1. **Equivalent Diameter:** Equivalent diameter is the diameter of a circle having the same area as the detected pore.

Mathematically:

$$D_{eq} = \sqrt{\frac{4A}{\pi}}$$

Where:

D_{eq} = equivalent diameter

A = pore area

2. **Shape Factor:** This describes how close a pore shape is to a perfect circle.

Mathematical Definition

Most commonly:

$$SF = \frac{4\pi A}{P^2}$$

Where:

SF = shape factor

A = pore area

P = pore perimeter

3. **Anisotropy:** This measures the directional preference of pore orientation. MIPAR usually computes anisotropy using:

- inertia tensor
- structure tensor
- eigenvalue decomposition

Conceptually: If λ_1, λ_2 are principal eigenvalues, anisotropy is related to their ratio.

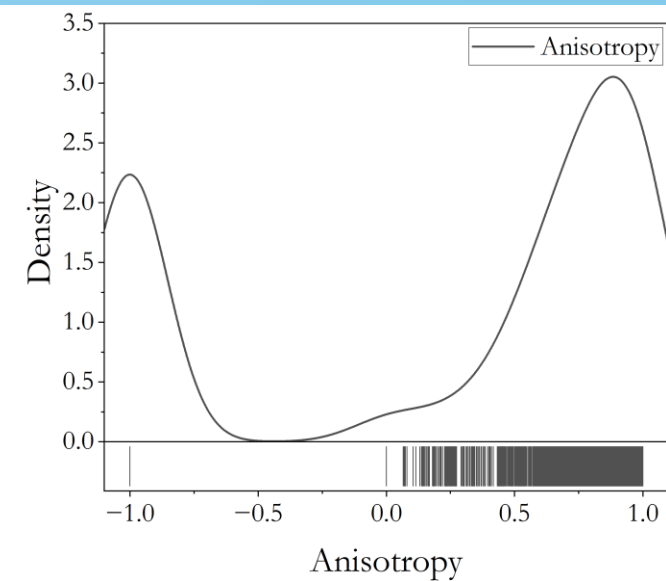
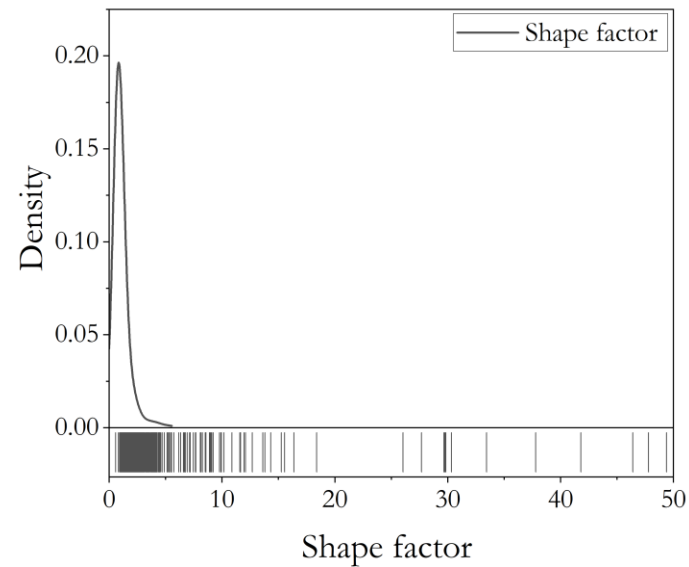
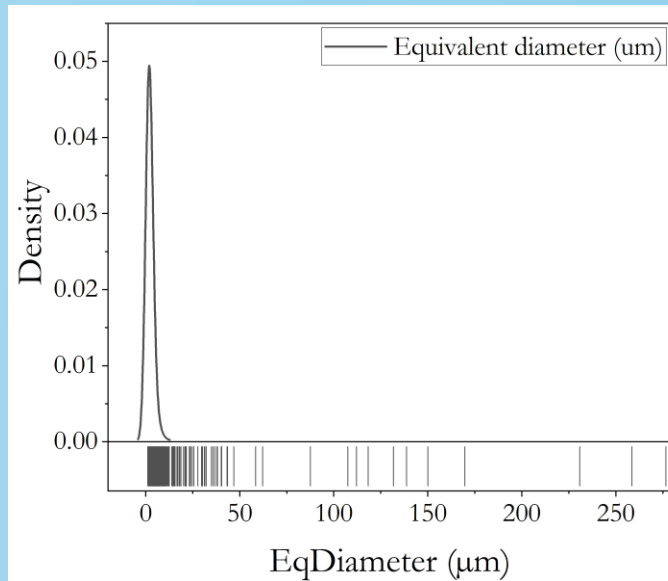
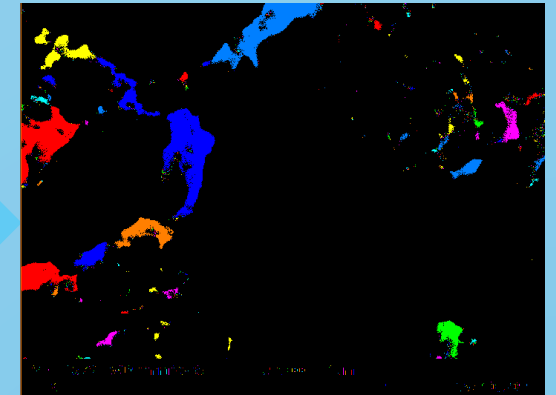
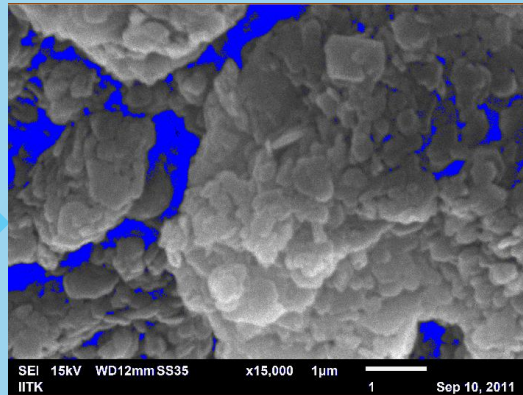
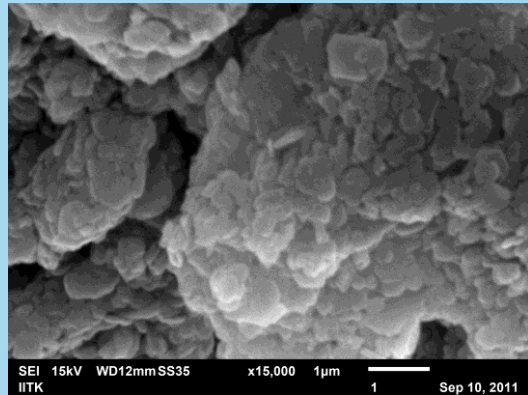
For isotropic pores:

$$\lambda_1 \approx \lambda_2$$

For elongated directional pores:

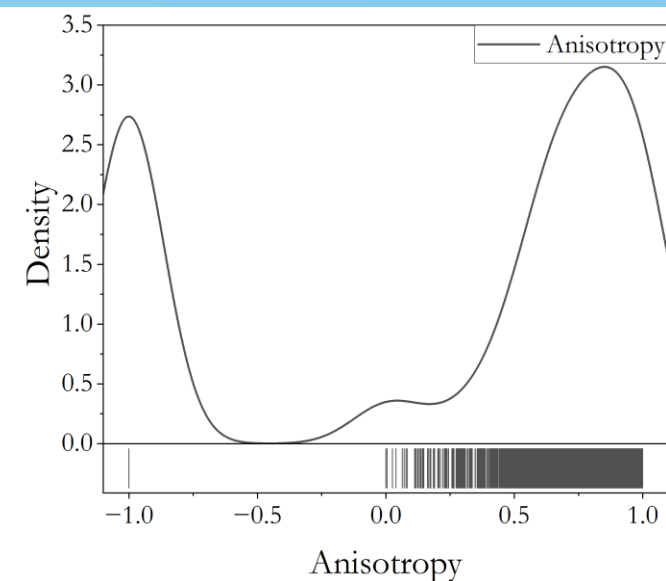
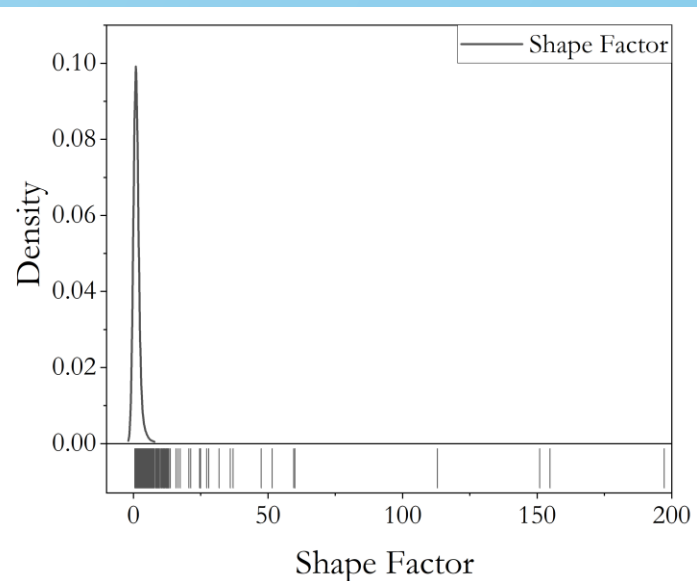
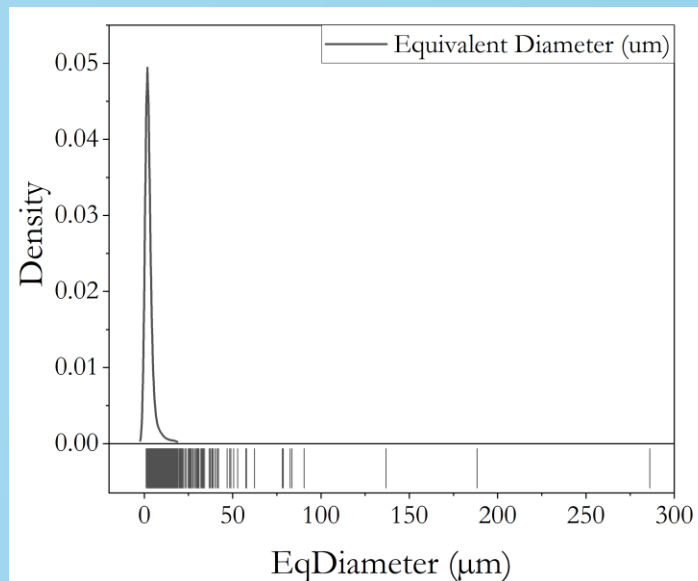
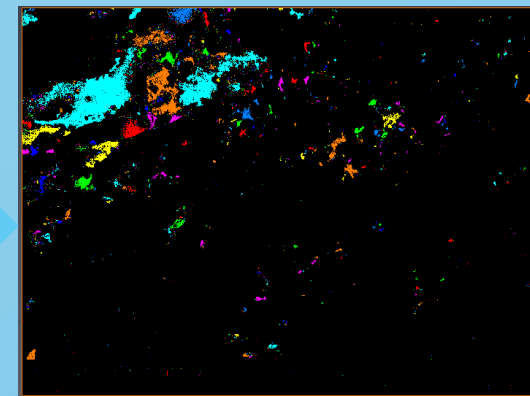
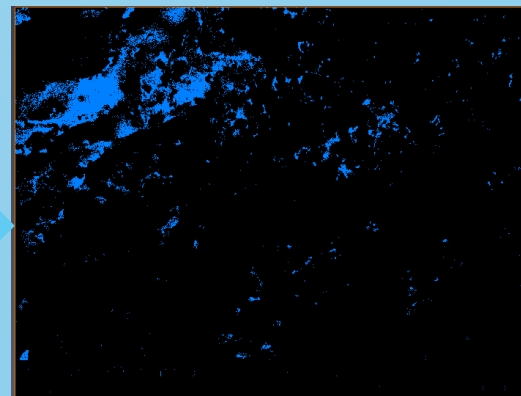
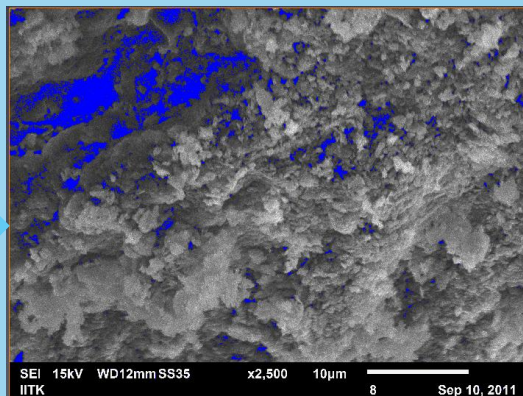
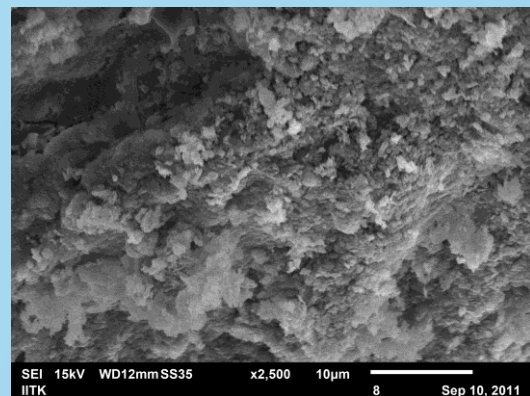
$$\lambda_1 \gg \lambda_2$$

RESULTS: S1_I1 + 2ml Ethyl alcohol



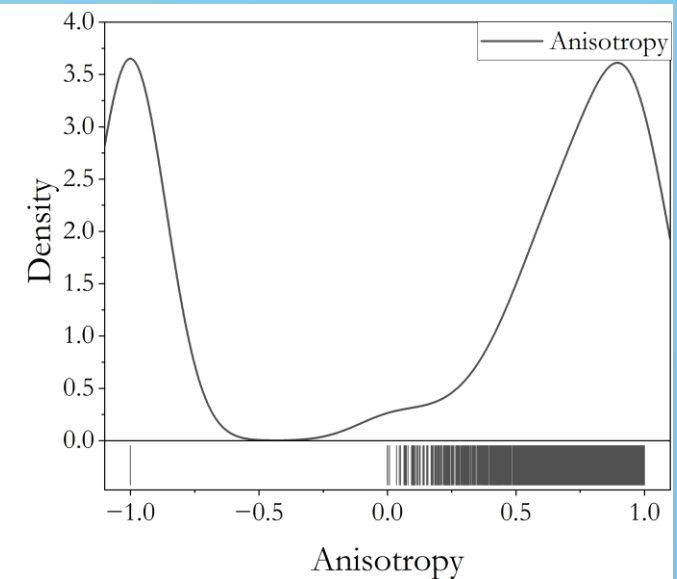
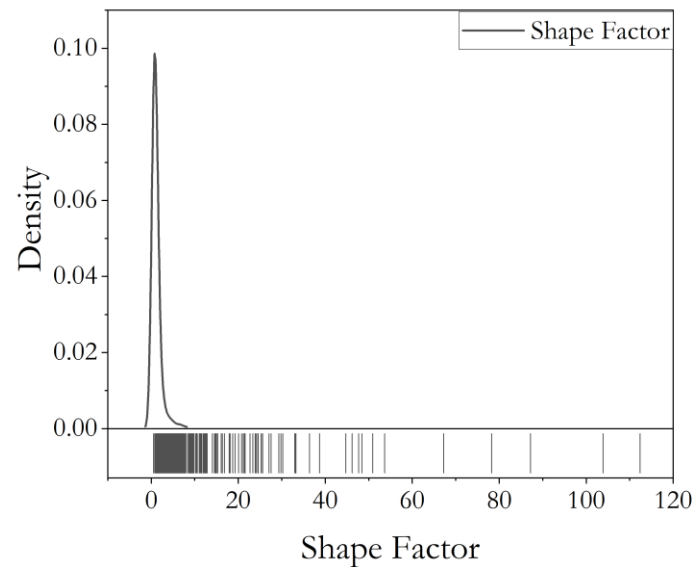
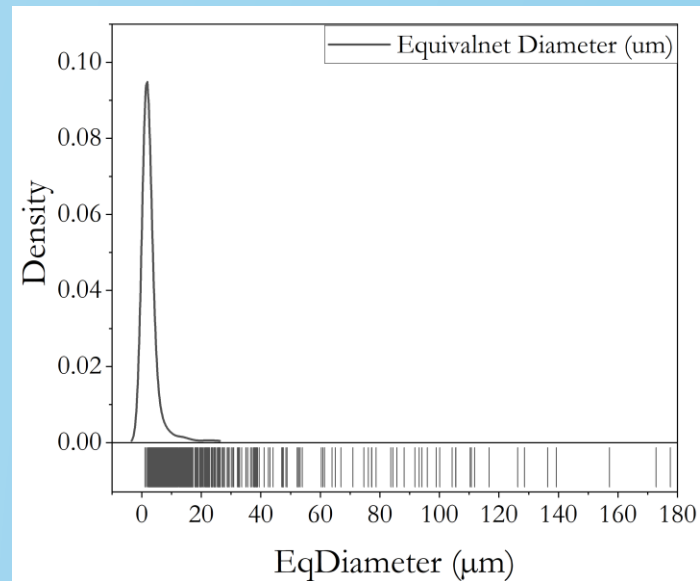
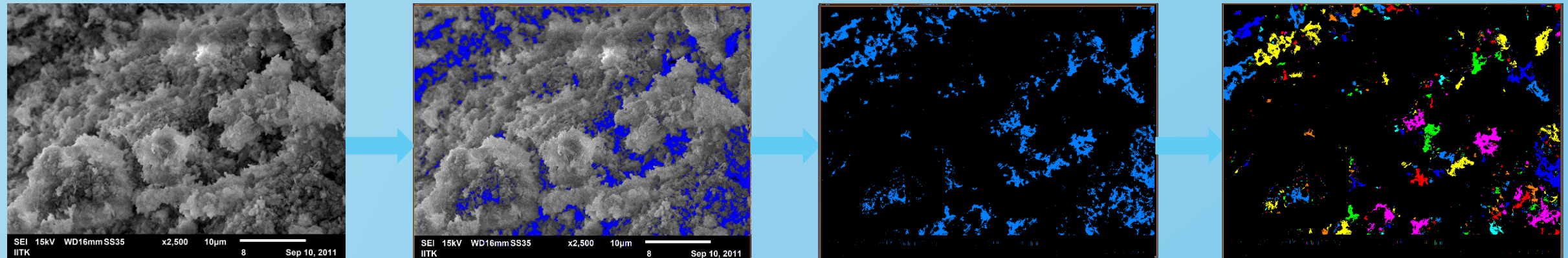
BENTONITE: 24 hours air dry, loaded to 1kg for 48 hours, water content= 12.62%

RESULTS: S2_I4 + 2 ml Ethyl alcohol



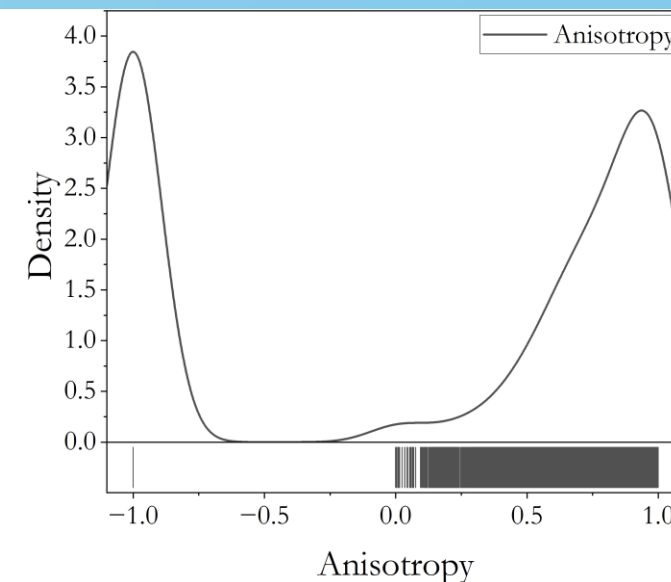
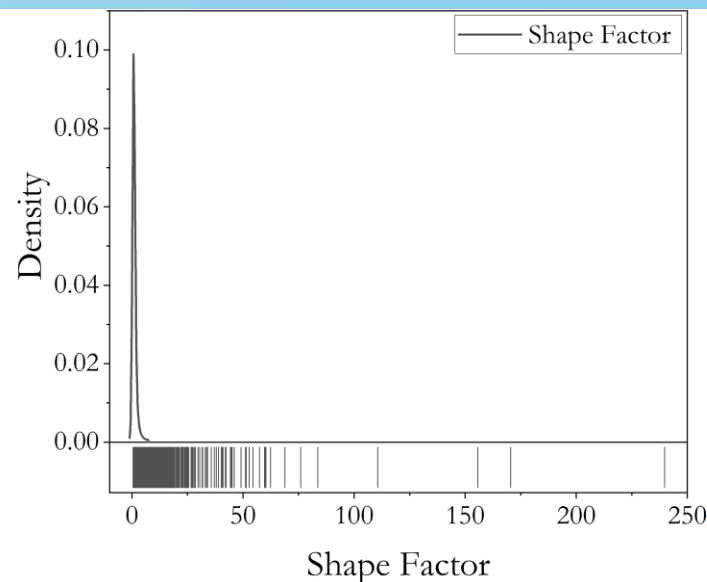
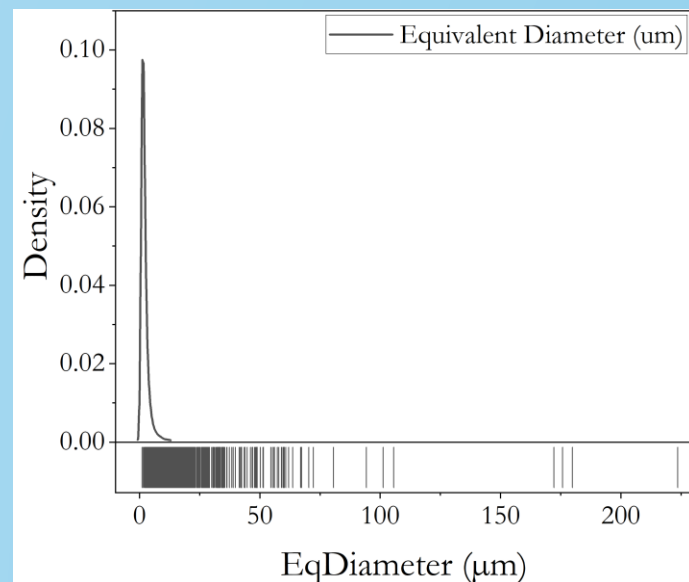
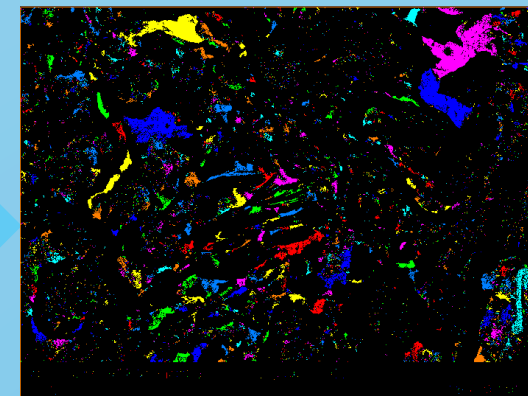
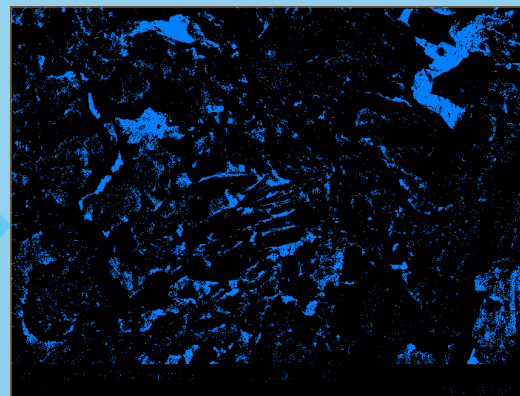
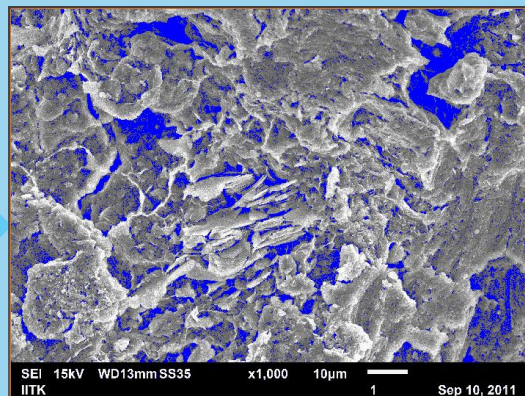
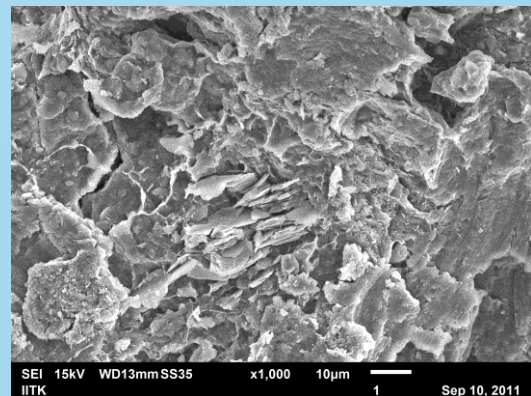
BENTONITE: 48 hours air dry, loaded to 1kg for 48 hours, water content= 10.34%

RESULTS: S3_I3 + 2 ml Ethyl alcohol



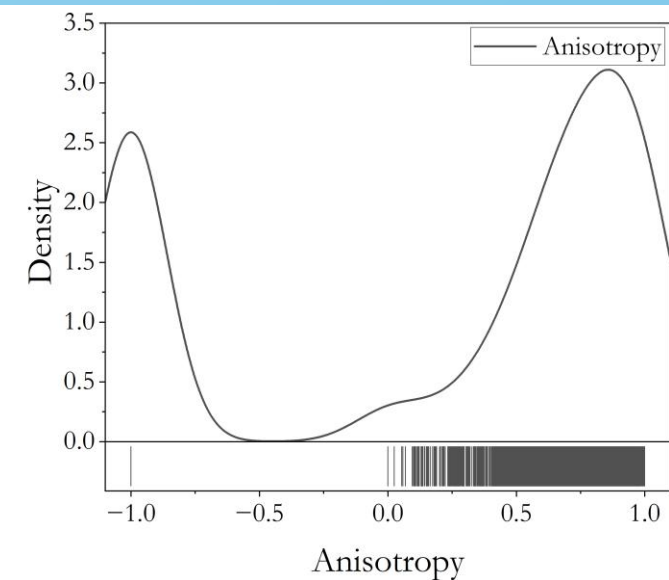
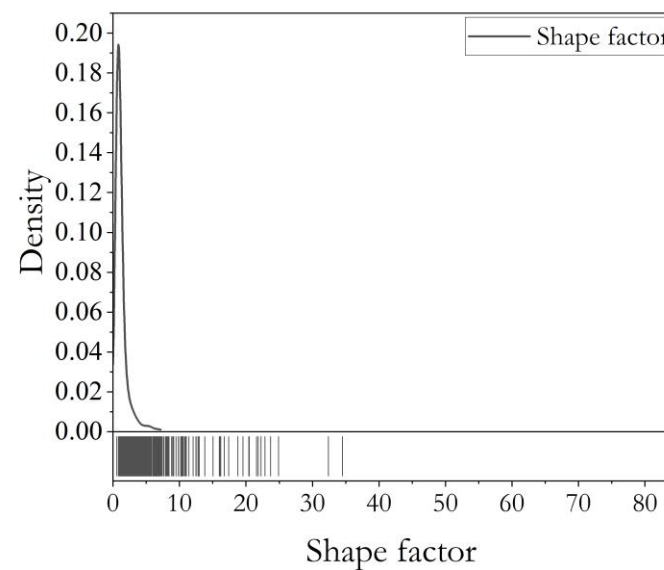
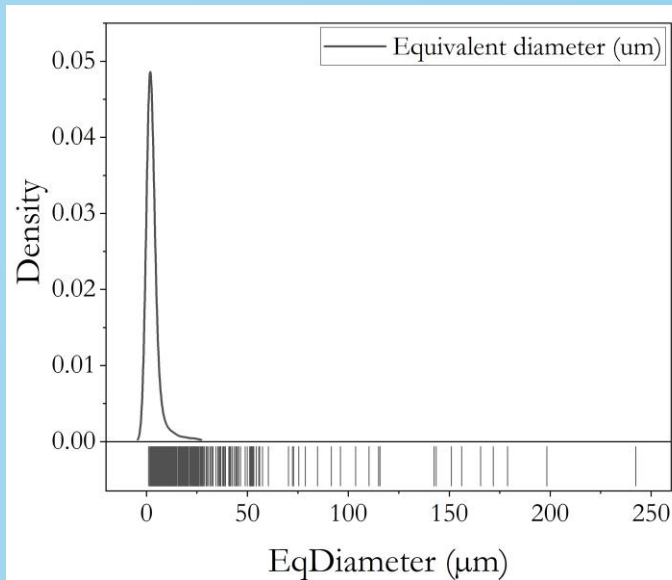
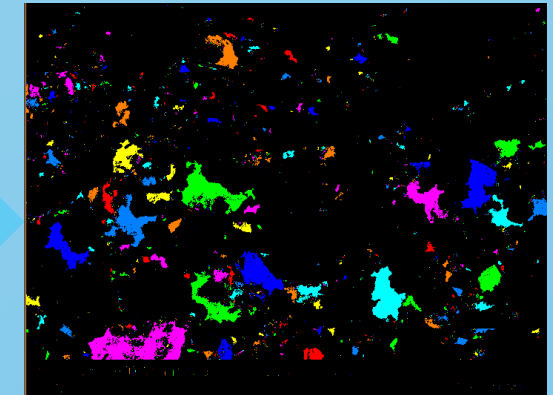
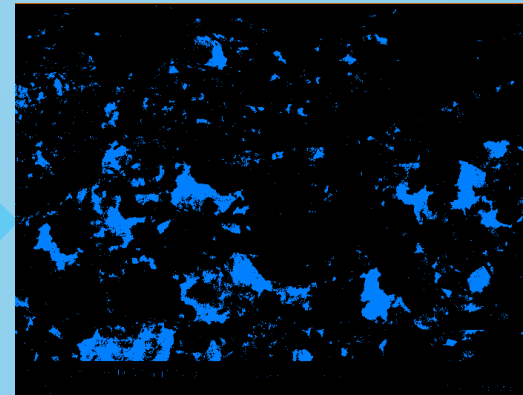
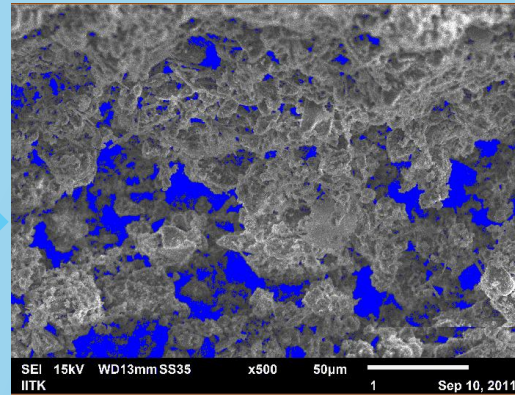
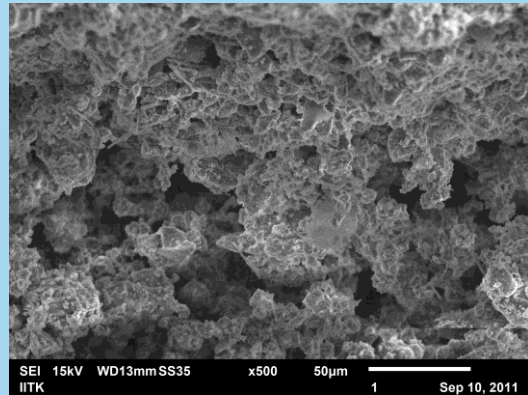
KAOLONITE: 24 hours air dry, loaded to 0.5 kg for 48 hours, water content= 7.8%

RESULTS: S4_I5 + 2 ml Ethyl alcohol



KAOLONITE: 48 hours air dry, loaded to 0.5 kg for 48 hours, water content= 7.2%

RESULTS: S6_I2



80% KAOLONITE+20 % SAND: 48 hours air dry, loaded to 0.5 kg for 48 hours, water content= 7.2%

Interpretation

The observed microstructural evolution suggests:

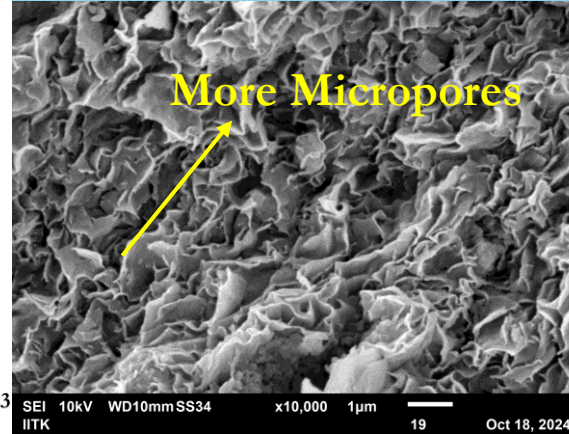
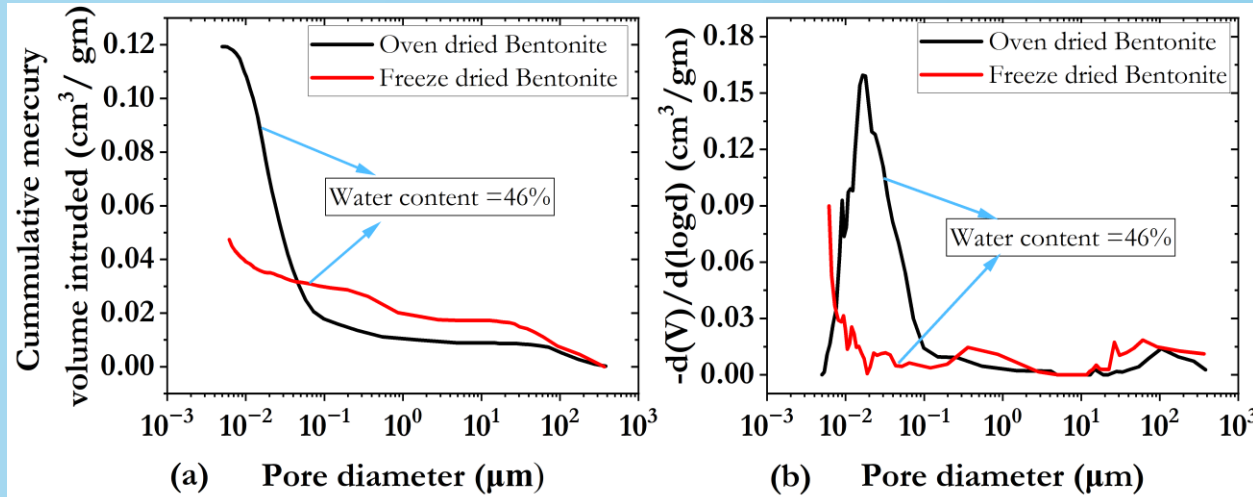
- gradual transition from micro-pores to macro-pores,
- increased pore coalescence,
- development of crack-like elongated voids,
- and enhanced directional connectivity of the pore system.

These changes may significantly influence:

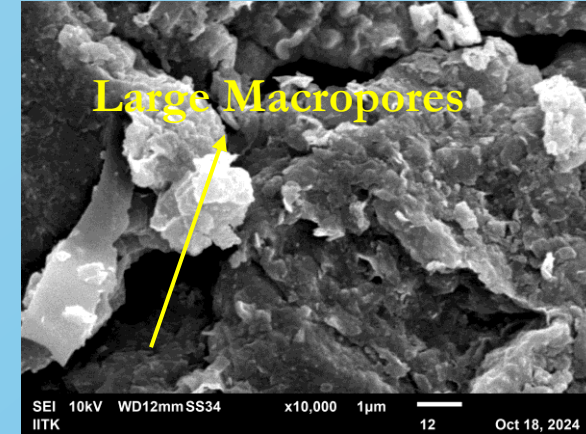
- permeability,
- compressibility,
- hydraulic conductivity,
- and long-term durability of fine-grained soils.

Sample	Pore Connectivity	Pore Irregularity	Macro-Pore Development	Anisotropy
S1_I1	Low	Low	Low	Moderate
S2_I4	Moderate	Moderate	Moderate	Moderate
S3_I3	Moderate–High	High	High	High
S4_I5	High	Very High	High	Very High
S6_I2	Very High	Very High	Very High	High

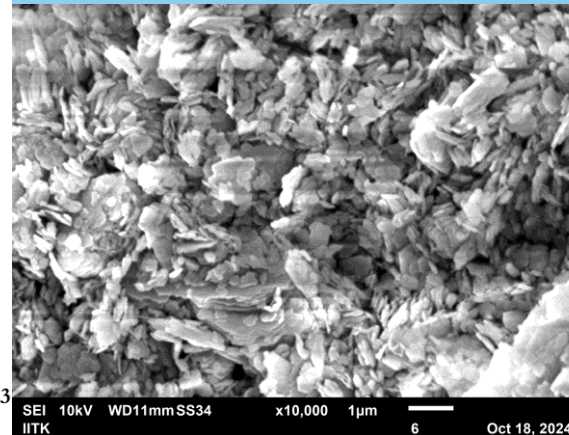
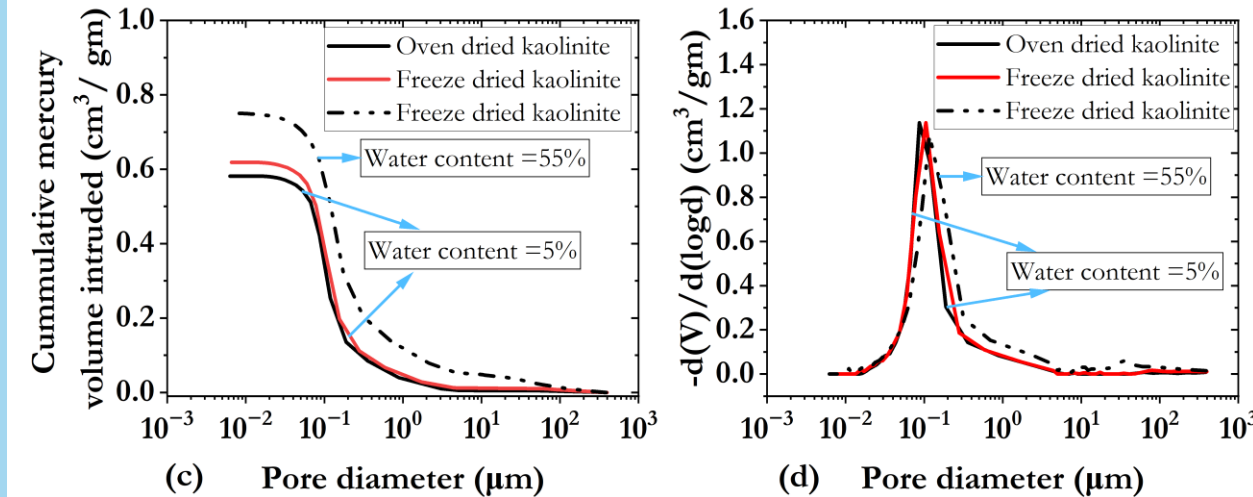
RESULTS:



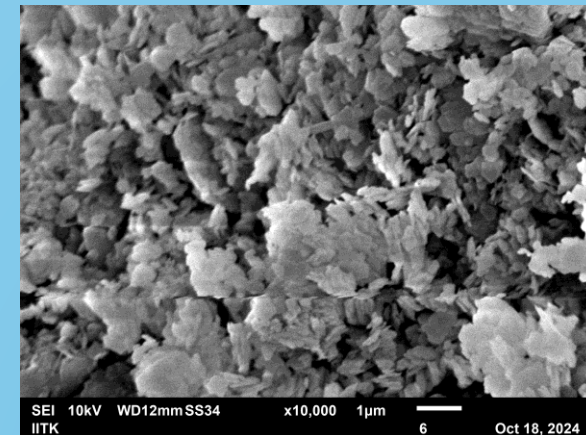
Oven-dried bentonite



Freeze-dried bentonite



Oven-dried kaolinite



Freeze-dried kaolinite

Fig. (a),(c) Cumulative pore size distribution and (b),(d) Pore size distribution

Fig. SEM images of bentonite and kaolinite

RESULTS:

- Two lognormal distribution functions are superimposed to obtain a bimodal particle size distribution (PSD).

$$f_B (d) = \frac{a_1}{\sqrt{2\pi} \sigma_1 d} e^{-[(\log d - u_1)^2]/2\sigma_1^2} + \frac{a_1}{\sqrt{2\pi} \sigma_2 d} e^{-[(\log d - u_2)^2]/2\sigma_2^2}$$

Inter-PSD function **Intra-PSD function**

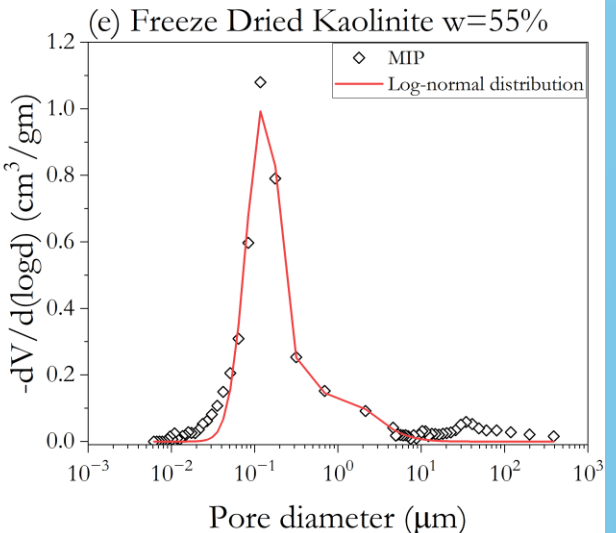
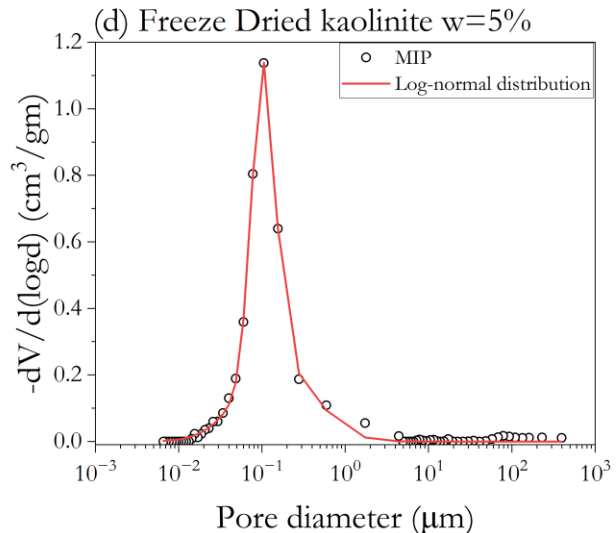
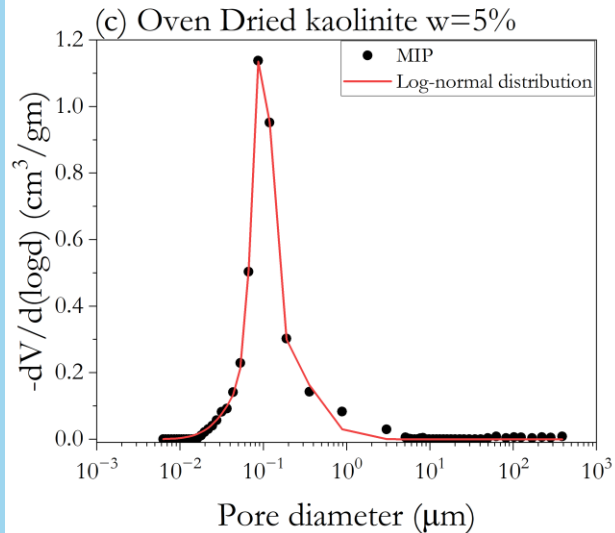
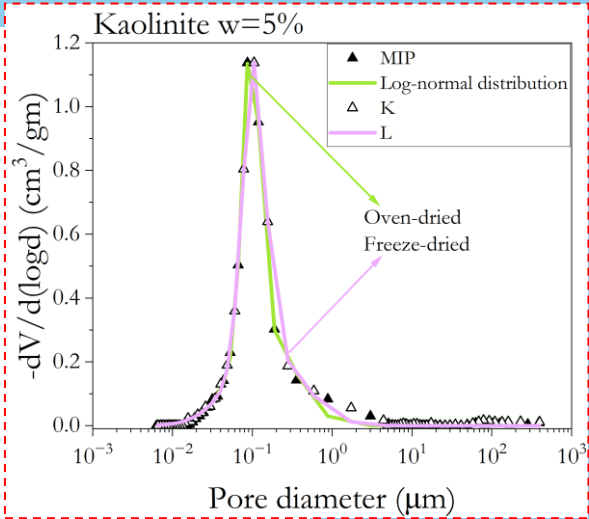
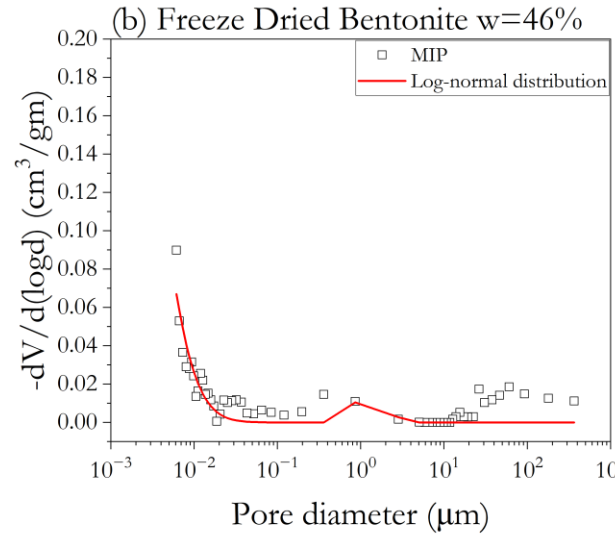
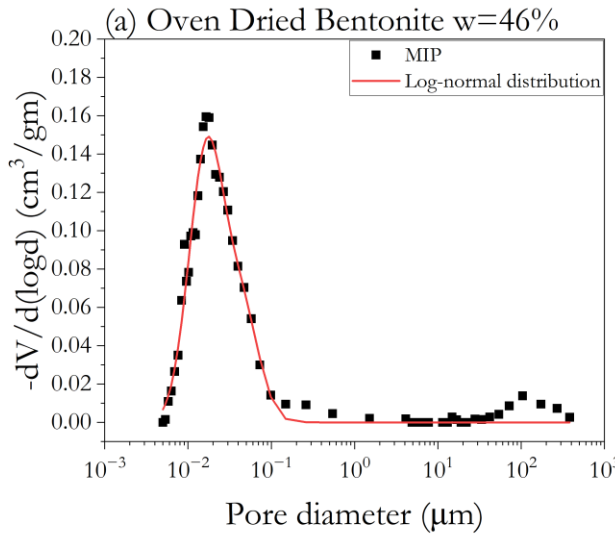
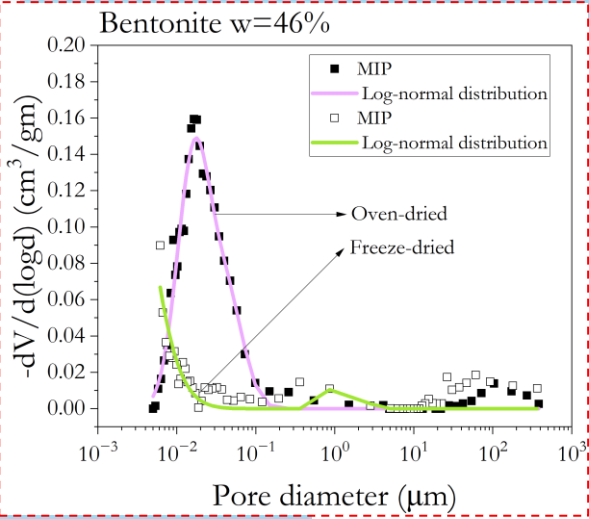
Where these **inter** and **intra PSD** can be explicitly given by:

$$a_1 f_1(\log(d)) = \frac{a_1}{\sqrt{2\pi} \sigma_1 d} e^{-[(\log d - u_1)^2]/2\sigma_1^2}$$

$$a_2 f_2(\log(d)) = \frac{a_1}{\sqrt{2\pi} \sigma_2 d} e^{-[(\log d - u_2)^2]/2\sigma_2^2}$$

Soil sample	a_1	μ_1	σ_1	a_2	μ_2	σ_2
Oven dry bentonite 46%	0.0031	-2.8786	0.4577	0.0034	-3.8429	0.4928
Freeze dry bentonite 46%	0.2187	0.4369	0.2129	0.0013	-5.7876	1
Oven dry kaolinite 5%	0.1311	-1.2409	0.8735	0.0572	-2.2827	0.2405
Freeze-dry kaolinite 5%	0.1482	-0.9031	1	0.0785	-2.1701	0.3155
Freeze-dry kaolinite 55%	0.5245	0.8486	1	0.1688	-1.8328	0.4769

RESULTS:





REFERENCES:

1. Chuhan, F. A., Kjeldstad, A., Bjørlykke, K., & Høeg, K. (2002). Porosity loss in sand by grain crushing—Experimental evidence and relevance to reservoir quality. *Marine and Petroleum Geology*, 19(1), 39-53. [https://doi.org/10.1016/S0264-8172\(01\)00049-6](https://doi.org/10.1016/S0264-8172(01)00049-6)
2. Fu, J., Thomas, H. R., & Li, C. (2021). Tortuosity of porous media: Image analysis and physical simulation. *Earth-Science Reviews*, 212, 103439. <https://doi.org/10.1016/j.earscirev.2020.103439>
3. Thyagaraj, T., & Julina, M. (2019). Effect of pore fluid and wet-dry cycles on structure and hydraulic conductivity of clay. *Géotechnique Letters*, 9(4), 348-354. <https://doi.org/10.1680/jgele.19.00046>
4. de Oliveira, J. A., Cássaro, F. A., & Pires, L. F. (2021). Estimating soil porosity and pore size distribution changes due to wetting-drying cycles by morphometric image analysis. *Soil and Tillage Research*, 205, 104814. <https://doi.org/10.1016/j.still.2020.104814>
5. Ma, T., Wei, C., Yao, C., & Yi, P. (2020). Microstructural evolution of expansive clay during drying–wetting cycle. *Acta Geotechnica*, 15, 2355-2366. <https://doi.org/10.1007/s11440-020-00938-4>.
6. Yu, B., Fan, W., Dijkstra, T. A., Wei, Y. N., & Deng, L. S. (2022). Pore structure evolution due to loess collapse: A comparative study using MIP and X-ray micro-CT. *Geoderma*, 424, 115955. <https://doi.org/10.1016/j.geoderma.2022.115955>
7. An, R., Kong, L., Zhang, X., & Li, C. (2022). Effects of dry-wet cycles on three-dimensional pore structure and permeability characteristics of granite residual soil using X-ray micro computed tomography. *Journal of Rock Mechanics and Geotechnical Engineering*, 14(3), 851-860. <https://doi.org/10.1016/j.jrmge.2021.10.004>
8. Li, K. P., Chen, Y. G., Ye, W. M., & Wang, Q. (2023). Modelling the evolution of dual-pore structure for compacted clays along hydro-mechanical paths. *Computers and Geotechnics*, 157, 105308. <https://doi.org/10.1016/j.compgeo.2023.105308>
9. Yang, J. W., Cui, Y. J., Mokni, N., & Ormea, E. (2024). Investigation into the mercury intrusion porosimetry (MIP) and micro-computed tomography (μ CT) methods for determining the pore size distribution of MX80 bentonite pellet. *Acta Geotechnica*, 19(1), 85-97. <https://doi.org/10.1007/s11440-023-01863-y>.



THANK YOU



Supervisor:

Professor Arghya Das

FB 304, Department of Civil Engineering

Indian Institute of Technology Kanpur

T: +91 512 259 6978

Email- arghya@iitk.ac.in